

# Gas Mixing in a Square Duct

EUGENE MILLER, S. P. FOSTER, R. W. ROSS, and KURT WOHL

There are numerous practical examples of the importance of gas mixing to the chemical industry and to combustion-engine technology. In the chemical plant good mixing is often a criterion for obtaining profitable yields. In the Diesel and Otto cycle engines, gas turbines, rockets and ramjets, gas mixing has an important bearing on performance. Moreover, poor mixing often causes excessive corrosion or erosion of reactor and combustion chamber walls because of the presence of zones of extreme temperature or chemical concentration.

A number of theoretical and experimental investigations have been reported on the mixing of free and coaxial jets (5, 9 to 12). These studies frequently do not apply to the more complicated mixing conditions encountered in industry.

Chilton and Genereaux (4) introduced a sidestream gas containing smoke into a gas mainstream and studied the resultant mixing process visually. They concluded that an ordinary  $T$  configuration gave as good mixing as any other simple arrangement having low energy requirements and that the mass velocity ratio of the two gas streams was the controlling variable.

More recently, in a series of papers (1, 2, 3, 13, 14), Callaghan, Ruggeri, and Bowden studied the penetration of a hot-air jet into an air stream flowing perpendicular to it in a narrow, high channel. They followed the limits of jet penetration into the channel by means of a thermocouple rake and measured temperature profiles for various relative angles of the sidestream and for different sidestream-orifice shapes. A jet emerging from a square orifice penetrated further into the channel than one emerging from a circular orifice of the same cross-sectional area.

Ehrich (6) analyzed the dynamics of jets entering into a general stream at an oblique angle from slots and orifices, based on simplified two-dimensional potential-flow theory. His study agreed qualitatively with Callaghan and Ruggeri's penetration data (1). Frazer (7) made a complementary, three-dimensional potential-flow analysis of a round jet penetrating into a main stream at right angles and also obtained qualitative agreement with Callaghan and Ruggeri.

Hawthorne, Rogers, and Zaczek (8) studied the penetration and mixing of a jet of cold air issuing through a hole in the wall of a 3-in.-square duct carrying hot air. This work came to the authors' attention after completion of the present work. Measurements were made with a temperature rake

with some complementary shadowgraph and schlieren photographs. The duct length required to obtain the same degree of mixing in a 3-in.-square duct was found to be twice that in a 1½-in.-square duct. A correlation of the distance to which the cold jet penetrated the hot air in the main duct was obtained with the factor  $R_m R_v / (1 + R_v)^2$  in terms of the present nomenclature. Turbulence in the hot stream reduced the penetration. Also, the penetration increased if another jet or a rod was placed immediately upstream. A jet emerging from a square hole penetrated as far into the duct as did a jet from a circular hole of equal area. A jet emerging from a rectangular hole of the same area penetrated further into the duct when placed with its long side in the direction of the stream and less when placed transversely.

The present study is an extension of the work initiated by Chilton and Genereaux. The characteristics and controlling parameters of gas mixing in a square duct with a sidestream entering at right angles have been examined more completely by means of instantaneous shadow photography and chemical-sampling techniques. It has been possible to obtain a semiquantitative picture of gas mixing under this circumstance which may have application to industrial problems.

## SCOPE OF WORK

The main experimental situation chosen for study was the mixing of an air stream flowing in a square duct with a stream of carbon dioxide entering from the side. The sidestream tube was placed perpendicular to the main duct with the exit port ending flush with the main duct inner wall. In a small number of tests the roles of the gases were inverted.

For flow visualization of the mixing process, instantaneous shadow photographs were found superior to smoke photography and chemical or thermal analysis. Although basically a qualitative tool as used, the instantaneous shadowgraph was found unexcelled in its revelation of the turbulent structure of mixing. Measuring on the shadowgraph the distance to which mixing had progressed to some defined degree made it possible to obtain quantitative results as well. Sampling by means of a probe yielded results which were in good agreement with the conclusions drawn from the shadowgraphs.

The following parameters and experimental variables were independently and systematically varied:

1. Main duct size  $D$ , 1-, 2-, and 3-in. square
2. Main-gas-stream velocity,  $V_D$ , 12.5 to 100 ft./sec.
3. Sidestream: main-stream mass velocity ratio  $R_m$ , 2 : 1 to 32 : 1
4. Sidestream: main-stream volume flow ratio  $R_v$ , 1 : 50 to 1 : 1.6
5. Sidestream port shape—circular, square, and rectangular (length : width ratio of 1.9 : 1). Also, slits extending over the whole width of the main duct were used.

All possible combinations of the variables however, were not explored. Reference is made to the experimental results for details.

## CRITERIA FOR MIXING

A typical example of mixing is shown in the instantaneous shadowgraph, Figure 1. Air is flowing horizontally in the 3-in.-square main duct at a velocity of 49 ft./sec. with carbon dioxide entering sideways at the bottom wall from a cylindrical tube.  $R_m$  is 4.6 and  $R_v$  is 1 : 12.2. Typically for these conditions, the entering carbon dioxide jet first is bent by the mainstream, then spreads, reaches the opposite duct wall, distributes itself across the duct more or less evenly, and finally blends completely with the main stream.

After an examination of shadowgraphs taken for various mixing conditions, four parameters were chosen as descriptive of the mixing process. These can be understood from Figure 1.

*Penetration distance  $P$*  is defined as the longitudinal distance between the upstream edge of the sidestream-jet shadow image at the side tube port and the plane where the jet shadow just reaches the opposite wall. This parameter is a measure of the "stiffness" of the sidestream jet or its resistance to being bent. It is related to the problem of distributing the sidestream over the cross section of the duct. Penetration is the first requirement for complete mixing of the two streams. Penetration distance, as defined here, is different from the penetration described by Callaghan et al. and Hawthorne et al. These authors measured the transverse distance to the outer edge of the sidestream jet from the bottom wall of the main duct as a function of the

E. Miller is at present with Redstone Arsenal, Huntsville, Alabama; S. P. Foster with E. I. du Pont de Nemours Company, Inc., Wilmington, Delaware; R. W. Ross with Shawinigan Resins Corporation, Springfield, Massachusetts; and Kurt Wohl at the University of Delaware, Newark, Delaware.

distance down the main duct from the sidestream inlet.

**Bulk mixing distance  $B$**  is defined as the longitudinal distance between the center of the side tube port and the plane where the schlieren are distributed (but not necessarily uniformly) over the whole duct. At this distance, bulky and nonuniform schlieren are visible. The bulk mixing distance is at least as large as the penetration distance but is usually larger.

**Macromixing distance  $M$**  is defined as the longitudinal distance between the center of the side tube port and the plane where a roughly even distribution of the schlieren is accomplished over the cross section of the duct. The schlieren intensity and scale, i.e., "graininess," are uniform over the cross section at this distance. Coarse mixing has been accomplished, but molecular mixing has not yet been completed. Molecular mixing also takes place during this interval, but macrodistribution is the dominant operation. The macromixing distance is at least as long as the bulk mixing distance but is usually longer.

**Micromixing distance**, to be consistent, should be defined by the longitudinal distance from the center of the side tube port to a plane where the schlieren have become invisible. The shadowgraph method though capable of defining the scale of the schlieren, cannot accurately resolve the plane at which the schlieren have disappeared because of the secondary patterns superimposed by the glass walls of the duct. Instead of a distance parameter, a scale of grading the quality of micromixing has been chosen which provides a method for describing the micromixing in a semiquantitative manner.

**Grade A:** excellent; very faint schlieren present after 3.5 duct diam. and none at 7 duct diam.

**Grade B:** good; distinct schlieren at 3.5 diam. and none or faint at 7 diam.

**Grade C:** fair, medium-scale schlieren present at 7 duct diam.

**Grade D:** poor; bulky, large-scale schlieren at 7 duct diam.

It would be difficult to ascertain the difference between the micro- and macromixing by another method such as chemical analysis. It is a virtue of the shadowgraph method to be able to discriminate between the two.

Shadowgraphs taken through the top and bottom duct walls (both of glass) and probe samplings indicated that the sidewise spreading and mixing of the sidestream jet with the main stream were completed before completion of the mixing viewed from the side. This was the case in all duct sizes studied. Since the side plane thus represented the controlling plane of mixing, the major portion of the shadowgraphs were taken in this plane.



(A)



(B)

Fig. 1. Mixing of air flowing in a 3-in. square duct with carbon dioxide entering sidewise from tube.  $R_v = 1:12.2$ ,  $R_m = 4.6$ ,  $V_D = 49$  ft./sec.

A. Upstream section, 0 to 2.3 duct diam. B. Downstream section, 2.3 to 4.6 duct diam.

#### ANALYSIS

Qualitative consideration of the mixing problem predicts that mixing is largely controlled by the size of the duct and side port and by the velocities and densities of the mainstream and sidestream jet. Viscous-force effects have been neglected.

For penetration distance  $P$ , there can be written:

$$P = f(D, d, V_D, u, \rho_D, \rho_d) \quad (1)$$

If

$$\frac{P}{D} = K_p \left( \frac{V_D}{u} \right)^a \left( \frac{D^2}{\pi d^2/4} \right)^b \left( \frac{\rho_D}{\rho_d} \right)^c \quad (2)$$

then

$$\frac{P}{D} = K_p \left( \frac{V_D \rho_D}{u \rho_d} \right)^{a-b} \left( \frac{V_D D^2}{u \pi d^2/4} \right)^b \left( \frac{\rho_D}{\rho_d} \right)^{c-a+b} \quad (3)$$

or

$$\frac{P}{D} = K_p \frac{(\rho_D/\rho_d)^\gamma}{R_m^\alpha R_v^\beta} \quad (4)$$

where

$$R_m = u \rho_d / V_D \rho_D \quad \text{and} \quad R_v = \frac{u \pi d^2/4}{V_D D^2}$$

The ratio  $D/d$  was a dependent variable in these experiments, since  $R_m$  and  $R_v$  were varied independently; by definition,

$$R_m = \frac{\rho_d}{\rho_D} \left( \frac{D^2}{\pi d^2/4} \right) R_v \quad (5)$$

Similarly,

$$\frac{B}{D} = \frac{K_b (\rho_D/\rho_d)^\delta}{R_m^\alpha R_v^\epsilon} \quad (6)$$

and

$$\frac{M}{D} = \frac{K_m (\rho_D/\rho_d)^\eta}{R_m^\alpha R_v^\epsilon} \quad (7)$$

It may be mentioned at this point that, at least for small ducts,  $\gamma = \delta = \eta = 0$ ; i.e., the effect of density ratio is taken care of by the term  $R_m$ .

The quality of micromixing is necessarily affected by the mass velocity and volume flow ratios since penetration, bulk mixing, and macromixing take place before completion of micromixing. However, final micromixing is molecular in nature and such factors as diffusivity would have to enter into the analysis as well. Since micromixing could be graded only qualitatively, no correlation was attempted.

#### APPARATUS AND PROCEDURE

Three different mixing chambers were used. They were square wooden ducts 1 in. square by 36 in. long, 2 in. square by 55 in. long, and 3 in. square by 85 in. long, with two side walls of special plate glass, Libby-Owens-Ford OS 1076. The 1- and 2-in. square ducts had glass walls for the last 20 in. of length, the 3-in. square duct for 39 in. Provision was made for introducing the mainstream gas into one end of the square duct and for the sidestream gas to enter through the bottom wall near the beginning of the glass-walled section, equidistant from the two side walls.

The flow length before the glassed section

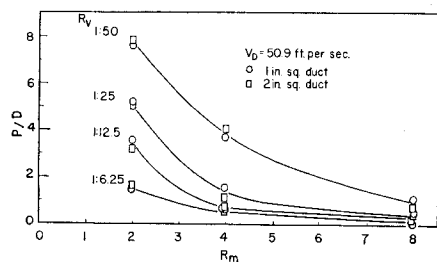


Fig. 2. Penetration distance: duct width as a function of mass velocity and volume flow ratios, 1- and 2-in. square ducts, cylindrical side tube.

of the 1- and 2-in. square ducts, 20 diam., was sufficient to smooth out entrance disturbances. The 3-in. square duct was somewhat short because of space limitations, 15 diam.; a 32-mesh screen was placed at the entrance to correct this deficiency. It was found experimentally, however, that flow disturbances produced at the entrance were negligible compared with the turbulence generated by the jet interaction.

The cylindrical tubes used for the side-stream were machined on a lathe. Rectangular and square tubes were formed from cylindrical brass tubes over previously machined mandrels. Dimensions of the various ports were measured with a traveling microscope.

The sampling probe consisted of a steel tube 0.047 in. I.D. by 0.004 in. wall by 12 in. long. Samples were withdrawn with the probe positioned parallel to the main gas stream. The holder was graduated in divisions of 0.01 in. for movement in horizontal and vertical directions perpendicular to the axis of the duct. The duct cross section was divided arbitrarily into nine equal sections, and for each sampling the probe was located at the center of a section. Samples were drawn into a burette with mercury as the working fluid. The sampling velocity through the probe was 25 ft./sec.

The sample was analyzed for carbon dioxide with a potassium hydroxide solution. A thin layer of water was kept on top of the mercury in the burette to keep the water-vapor content of the sample constant.

## EXPERIMENTAL RESULTS

### Shadowgraphic Studies

**Cylindrical Side Tube.** PENETRATION DISTANCE. In Figures 2 and 3,  $P/D$  measurements for the 1-, 2-, and 3-in. square ducts are correlated as a function of  $R_m$  and  $R_v$  at a main duct velocity of about 50 ft./sec. It may be seen that  $P/D$  decreases with an increase in  $R_m$  and  $R_v$ . At low values of  $R_m$  and  $R_v$ , e.g., 2 : 1 and 1 : 50 respectively, the carbon dioxide jet offers little resistance to the air stream and is swept down the duct for a relatively long distance before reaching the upper wall. At the highest values of  $R_m$  and  $R_v$  studied, e.g., 18 : 1 and 1 : 6.25 respectively, the sidestream jet offers so much resistance to the air stream that the penetration distance is almost zero. In between these extremes the penetration distance decreases continuously with increasing  $R_m$  and  $R_v$ .

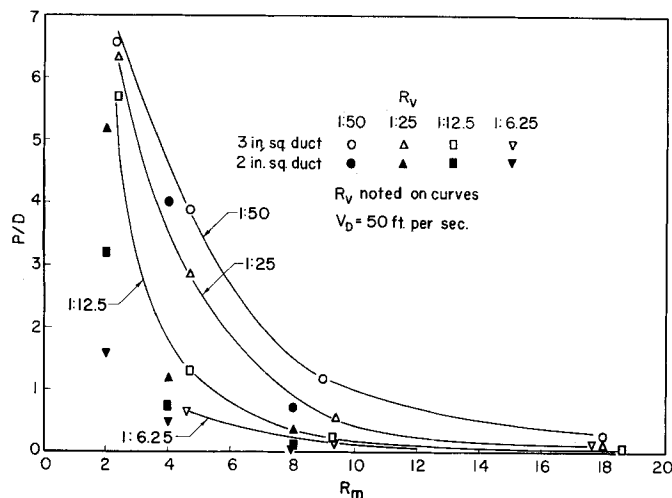


Fig. 3. Penetration distance: duct width as a function of mass velocity and volume flow ratios, 2- and 3-in. square ducts, cylindrical side tube.

In Figure 2 the data for both the 1- and 2-in.-square ducts are correlated by the same curves. Therefore, it may be concluded that  $P/D$  is independent of duct size in this range. In Figure 3 the data for the 3-in.-square duct are compared with the data for the 2-in.-square duct. It is evident that the values for the 3-in.-square duct are consistently higher.  $P/D$  is not independent of scale, therefore, above the 2-in.-square duct size.

In order to check on the validity of  $R_m$  and  $R_v$  as controlling variables for penetration distance, the roles of the gases were inverted in the 1-in.-square duct, carbon dioxide becoming the main-stream and air the sidestream. At this duct size at least, the data are correlated by  $R_m$  and  $R_v$  independent of the density of the gases. It was not possible to repeat these tests in the larger ducts because of limitations of the carbon dioxide supply.

The penetration distance data for all three ducts were correlated by

$$P/D = K_p/R_m^2 R_v \quad (4a)$$

the exponent of the density ratio  $\gamma$  being zero. Equation (4a) applies to a fixed duct velocity and duct size in which  $R_m$  and  $R_v$  are independently varied. The results of the correlation are shown graphically in Figures 4 and 5.

The values of  $K_p$ , given in Figure 5a, were obtained from the data by the method of least squares. The independence of both duct size and role of the gases in the 1- and 2-in.-square ducts is evident from the identical values of  $K_p$  obtained. At every duct velocity studied the  $K_p$  values for the 3-in.-square duct are larger than for the 1- and 2-in.-square duct. Generally, it is seen from the figure that  $K_p$  decreases with an increase in duct velocity, although for the 3-in.-square duct data a single value of

$K_p = 1.6$  adequately correlates all the data. In general, the duct velocity, compared with the other variables, has only a small effect on the penetration distance.

Equation (4a), with these values of  $K_p$ , correlates the results by approximately  $\pm 20\%$ . The largest deviations from the correlation are found for the smallest and largest values of  $P/D$ . At the smallest distances the relative error of measurement is, of course, large, and at the largest distances dilution effects make the measurements relatively doubtful.

Callaghan and Ruggeri's measurements of the "penetration" of air jets issuing from circular orifices into a 2- by 20-in. duct were correlated by

$$\left(\frac{l}{d}\right)^{1.65} = KR_m \left(\frac{S}{d}\right)^{0.5} \quad \text{in reference 1} \quad (8)$$

and as

$$\frac{l}{d} = K \left(\frac{\rho_d}{\rho_D}\right)^{0.52} \left(\frac{u}{V_D}\right)^{0.59} \cdot \left(\frac{S}{d}\right)^{0.26} \quad \text{in reference 3} \quad (9)$$

for large values of the ratio of the width of the jet to the orifice diameter  $d$ . In these correlations,  $l$  is the penetration and  $S$  is the distance downstream of the jet entrance at which penetration is measured. If special pairs of values of  $l$  and  $S$  are interpreted as  $D$  and  $P$  respectively, in terms of the present definition of penetration distance the following expressions result:

$$\frac{P}{D} = \frac{K_p (D/d)^{2.3}}{R_m^2} = \frac{K_p (\rho_D/\rho_d) (D/d)^{0.3}}{R_m R_v} \quad (8a)$$

and

$$\frac{P}{D} = \frac{K_p(D/d)^{2.3}}{R_m^2 R_v^{0.3}} =$$

$$\frac{K_p(\rho_D/\rho_d)(D/d)^{0.3}}{R_m R_v^{1.3}}, \text{ respectively } (9a)$$

The differences between these results and those of the present paper are due probably to differences in experimental configuration. Also, in the cited experiments the duct boundary layer was removed by suction upstream of the jet orifice to minimize wall boundary-layer effects. This was not done in this work.

**BULK MIXING DISTANCE.** A correlation of  $B/D$  as a function of  $R_m$  and  $R_v$  for the 2- and 3-in.-square ducts is shown in Figure 6. Nominal duct velocity is 50 ft./sec. Approximately the data for the 2- and 3-in.-square ducts may be represented by the same curve. Data taken with the 1-in.-square duct also fall quite close except for low mass velocity ratios near 2 : 1 where the values for the 1-in.-square duct are somewhat lower.  $B/D$  may be considered independent of duct size and density ratio within the range of these tests. It was found that the duct velocity has only a slight effect on the parameter  $B/D$ , apparently less than observed for  $P/D$ .

A logarithmic plot of  $B/D$  vs.  $R_m$  at constant  $R_v$  merely produces a family of nonlinear curves. Bulk mixing distance is not, therefore, a simple exponential function of mass velocity and volume flow ratios as was proposed by Equation (6).

**MACROMIXING DISTANCE,  $M/D$ .** Figure 7 is a plot of  $M/D$  as a function of  $R_m$  and  $R_v$  at a constant duct velocity of 50.9 ft./sec. for the 1- and 2-in.-square ducts. The points for both ducts are satisfactorily correlated by the same curves, an indication that  $M/D$  is independent of duct size in this scale.

This independence does not extend to the 3-in.-square duct, as is seen in Figure 8. The data for the 3-in.-square duct are mostly higher than for the 1- and 2-in.-square ducts. Further, at higher  $R_m$  and  $R_v$  ratios the entire pattern of variation of  $M/D$  is reversed. At  $R_m \leq 8$ ,  $M/D$  decreases with an increase in  $R_m$  and  $R_v$ , just as in the 1- and 2-in.-square ducts. At  $R_m \geq 14$ ,  $M/D$  increases with an increase in  $R_m$  and  $R_v$ . Shadowgraphs show that as the sidestream volume flow rate and velocity are increased, a portion of the sidestream gas tends to hover at the upper wall.

When the sidestream jet strikes the opposite wall with force, it spreads out forward, backward, and sidewise in the plane of the wall. When the sidewise-spreading gases meet the side walls, they flow down to the bottom wall and finally fill the whole duct. During this distribution process turbulent mixing is of course taking place—not only in the distributed gas, but, prior to wall colli-

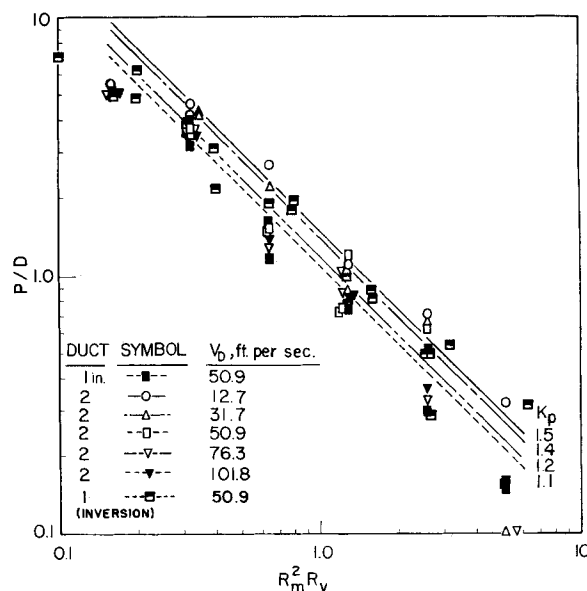


Fig. 4. Correlation of penetration distance: duct width with mass velocity and volume flow ratios, 1- and 2-in. square ducts, cylindrical side tube.

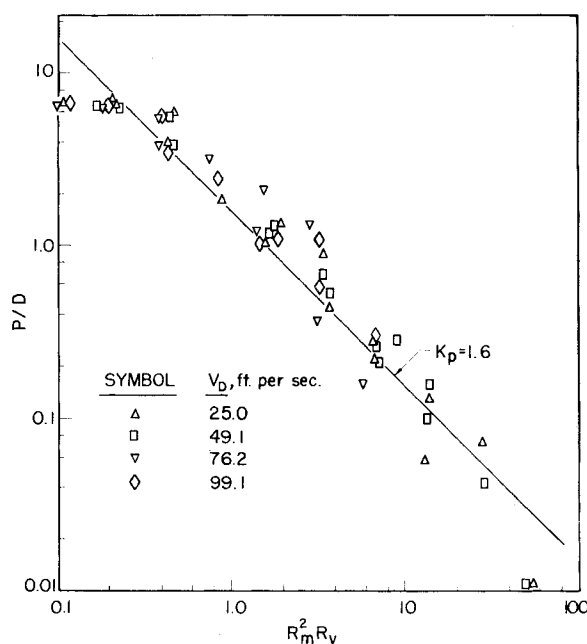


Fig. 5. Correlation of penetration distance: duct width with mass velocity and volume flow ratios, 3-in. square ducts, cylindrical side tube.

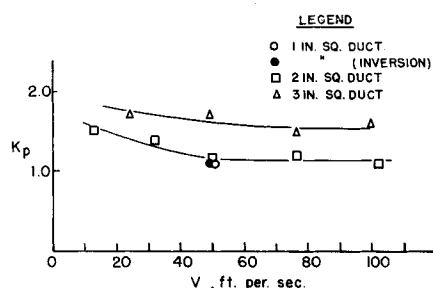


Fig. 5a.  $K_p$  as a function of duct velocity and duct size.

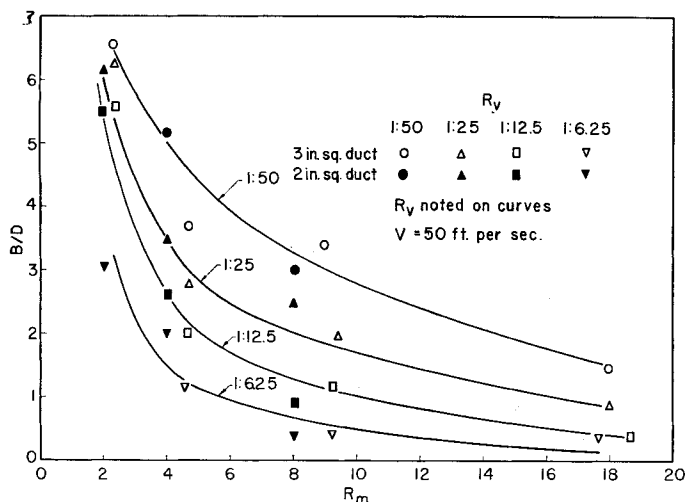


Fig. 6. Bulk mixing distance: duct width as a function of mass velocity and volume flow ratios, 2- and 3-in. square ducts, cylindrical side tube.

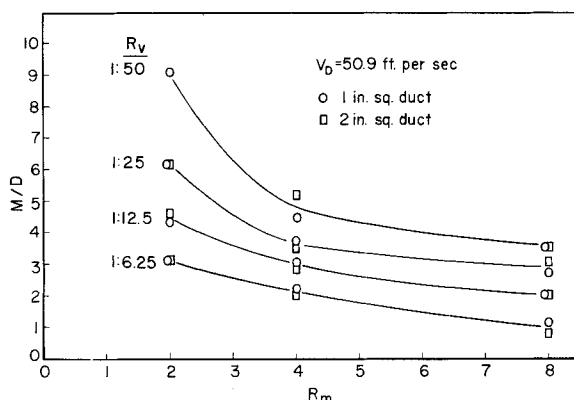


Fig. 7. Macromixing distance: duct width as a function of mass velocity and volume flow ratios, 1- and 2-in. square ducts, cylindrical side tube.

sion, in the jet as well. At higher  $R_m$  ( $> 8$ ) and  $R_v$  ( $> 1:25$ ) values, the sidestream jet collides with the opposite wall with great momentum, and mechanical distribution of the type described undoubtedly plays the larger part in macromixing. At smaller  $R_m$  and  $R_v$  values, turbulent mixing plays the more important role. The predominance of mechanical distribution effects at  $R_m > 8$  and turbulent mixing at  $R_m < 8$  probably accounts for the reversal of the variation of macromixing distance.

There is hardly any doubt that similar results would have been obtained with the smaller ducts if the experiments had been conducted for  $R_m > 8$ . See for example the results obtained for the rectangular side tubes, page 400.

The effect of density on  $M/D$  was studied in the 1-in.-square duct by inverting the roles of the air and carbon dioxide. The results for a duct velocity of 50.9 ft./sec. indicate that the  $M/D$  is independent of density ratio.

It was found that  $M/D$  data for the 1-

and 2-in.-square ducts could be correlated by

$$M/D = \frac{K_m}{(R_m R_v)^{1/2}} \quad (7a)$$

the exponent  $\eta$  of the density ratio being zero again, as in the case of penetration distance. Graphical representation of the correlation is shown in Figure 9.

The effect of main duct velocity on  $M/D$  is given in Figure 9a, where  $K_m$ , obtained from the data by means of the least squares method, is given as a function of the duct velocity, the effect of which is seen to be small. The  $K_m$  value in the 1-in.-square duct inversion study is slightly larger ( $\sim 6\%$ ) than the value found with air as the main duct gas. However, a  $K_m$  value of 1.7 can be used for correlating all the data in both 1- and 2-in.-square ducts within  $\pm 20\%$  with the exception of two points of questionable accuracy. For  $R_m > 8:1$  the equation does not describe the variation of  $M/D$  satisfactorily.

Correlation of the results for the 3-in.-square duct is shown in Figure 10. For this size of duct the equation

$$M/D = \frac{6.0}{R_m^{0.7} R_v^{0.2}} \quad (7b)$$

correlates the data for all the main duct velocities studied, 25 to 100 ft./sec., within  $\pm 25\%$ . The equation is valid for  $R_m \leq 18.5$  and for  $R_v \leq 1:25$ . For larger  $R_v$  values the correlation applies only to  $R_m \leq 8$ .

The exponents of  $R_m$  and  $R_v$  in Equation (7), then, vary for ducts larger than 2 in. square. In the 3-in.-square duct the effect of  $R_m$  is greater and the effect of  $R_v$  smaller than in the smaller ducts; i.e., the exponent of  $R_m$  increases and that of  $R_v$  decreases. Larger space, therefore, puts a premium on high momentum.

**QUALITY OF MICROMIXING.** The micromixing qualities were estimated for the 1-, 2- and 3-in. square ducts at a nominal main-duct air velocity of 50 ft./sec. For the 1-in.-square duct at  $R_v = 1:6.25$ , the quality of micromixing is  $D$  independent of  $R_m$  in the range 2 to 8. As  $R_v$  is increased to the range 1:12.5 to 1:50, the quality improves to  $C/D$  if an  $R_m = 8$  is used. The quality of micromixing for the 2-in.-square duct is the same as for the 1-in.-square duct except at  $R_v = 1:50$  and  $R_m > 2$ ; for  $R_m = 4$  and 8, the quality is  $C/D$  and  $C$  respectively. A large improvement in micromixing is observed for the 3-in.-square duct. At  $R_v = 1:6.25$  the quality of micromixing is  $D$ ,  $C/D$ , and  $A/B$  for  $R_m = 4, 8$ , and 16 respectively. At  $R_v = 1:12.5$  the quality is  $D$ ,  $C$ ,  $C$ , and  $B$  at  $R_m = 2, 4, 8$ , and 16 respectively. At  $R_v = 1:25$  and 1:50, the quality improves to  $D$ ,  $C$ ,  $B$ , and  $A$  corresponding to  $R_m = 2, 4, 8$ , and 16.

It may be seen that at constant  $R_v$ , the quality of micromixing improves with an increase in  $R_m$  and/or duct size. For a given  $R_m$  and duct size the quality of micromixing improves with a decrease in  $R_v$ . It is apparent also that  $R_m$  and duct scale have much stronger influences on the quality of micromixing than  $R_v$  does.

It was found in a study of the effect of main-duct air velocity on the quality of micromixing in the 3-in.-square duct that only small improvements in micromixing are obtained by an increase in duct velocity. However, an increase in duct velocity for a given  $R_m$  and  $R_v$  means an increase in the amount of material mixing and a shorter time in which to mix it for any given duct length. A small improvement in micromixing with increased duct velocity therefore takes on more significance. The same comment holds for bulk mixing and macromixing.

A definite improvement in micromixing is observed when the lighter gas forms the sidestream. When the roles of the

carbon dioxide and air are changed in the 1-in.-square duct, i.e. air is the side stream, at  $R_v$  from 1 : 12.5 to 1 : 50 the quality of micromixing is  $D$ ,  $C$ , and  $B$  for  $R_m = 2, 4$ , and  $8$  respectively. At  $R_v = 1 : 6.25$  the quality is  $D$ ,  $D$ , and  $B$  for the same values of  $R_m$ . These qualities may be compared with those given above for carbon dioxide as the sidestream. For micromixing, then, the sidestream jet velocity is the important factor, whereas penetration, bulk mixing, and micromixing depend on momentum. Qualitatively the effects of  $R_m$  and  $R_v$  in the inversion tests are similar to those found in the case where air is the mainstream.

**Opposed Cylindrical Side Tubes.** An obvious method of improving mixing is to introduce the sidestream gas from a number of opposed jets. A brief investigation was made, therefore, of mixing with two opposed sidestream jets. The results are summarized in Tables 1 and 2.

It is evident from the data that mixing takes place more rapidly with opposed jets than with a single sidestream jet. It may be noted that the reversal of the variation of  $M/D$  with  $R_m$  and  $R_v$  at  $R_m > 8$ , noted for single-jet mixing, is not observed with opposed jets.

If penetration distance is defined as the distance between the upstream boundary of the sidestream-jet shadow image at the side tube port and the plane where the schlieren of the two jets meet, the data in Table 1 indicate that penetration distance is decreased by more than the factor of two that might be expected from the symmetry of the arrangement. It appears that the reduction in tube diameter in the opposed configuration is responsible for reducing penetration distance further. Consequently, the two opposed jets impinge with greater momentum, and the turbulence produced results in mixing in a smaller duct length.

The data for  $M/D$  for the 1- and 2-in.-square ducts with opposed jets indicate shorter relative macromixing distances than for the 3-in.-square duct (Table 2). Thus the scale effect found for the single-jet mixing configuration appears to hold also for the opposed-jet configuration.

**Rectangular Side Tubes.** Although the bulk of the work was done with cylindrical side tubes, some study was made of the effect of jet shape and orientation. The studies were conducted in the 2-in.-square duct at a duct velocity of 50 ft./sec.

Rectangular tubes with length-width ratios of 1.9 were studied with orientations in which the short side of the tube was placed perpendicularly to the air stream and also with orientations in which the long side was placed perpendicularly. Square tubes were also studied.

When the sidestream enters through a tube the diameter of which is small compared with the width of the duct, the bulk of the main gas slips by the sidestream without contact. In order to

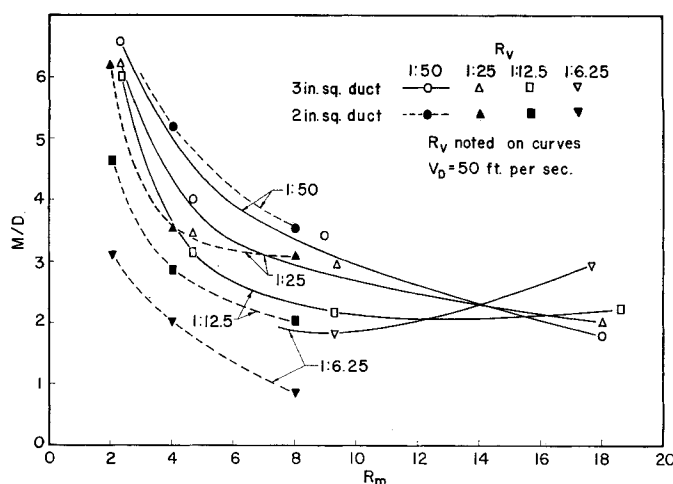


Fig. 8. Macromixing distance: duct width as a function of mass velocity and volume flow ratios, 2- and 3-in. square ducts, cylindrical side tube.

TABLE 1. OPPOSED JET STUDY

Three-in square duct, carbon dioxide entering sideways

Air velocity, ft./sec.	Volume flow ratio, CO <sub>2</sub> :air	Mass velocity ratio, CO <sub>2</sub> :air	Penetration distance/duct width		Bulk mixing distance/duct width		Macromixing distance/duct width		Quality of micromixing	
			Opposed Jets	Single Jet	Opposed Jets	Single Jet	Opposed Jets	Single Jet	Opposed Jets	Single Jet
50.1	1:50	7.45:1	0.26	1.7	2.10	3.5	2.30	3.5	B	B
50.1	1:50.5	3.74:1	1.26	5.2	1.61	4.8	2.30	4.8	B	C
50.1	1:50	1.93:1	2.13	6.6	2.10	6.6	3.70	6.6	C	D
50.1	1:50	0.97:1	3.83	6.6	3.83	6.6	4.60	6.6	C	D
50.1	1:25.7	14.50:1	0	0.1	0.40	1.3	1.24	2.3	A	B
50.1	1:25.5	7.42:1	0.11	1.1	1.23	2.2	1.24	3.1	B	B
50.1	1:25.4	3.81:1	0.61	3.8	1.30	3.4	2.30	4.7	C	C
50.1	1:25	1.92:1	1.43	6.6	1.35	6.6	2.30	6.6	C	D
50.1	1:13	14.60:1	0	0	0.29	0.6	0.31	2.2	A	B
50.1	1:12.5	7.75:1	0	0.4	0.88	1.3	1.34	2.4	A	C
50.1	1:12.7	3.81:1	0.425	2.0	0.70	2.6	2.83	4.4	C	C
50.1	1:6.25	7.75:1	0	0.3	0.64	0.6	0.88	1.9	A	C/D
12.7	1:50	7.41:1	0.32		4.60		4.60		C	
12.7	1:50	3.77:1	1.00		0.94		2.00		B	
12.7	1:25	7.51:1	0.16		1.37		2.30		B	
12.7	1:25	3.86:1	0.47		0.55		2.30		B	
12.7	1:12.8	14.75:1	0		0.26		0.65		A	


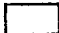


TABLE 2. OPPOSED JET STUDIES

Comparison of Data from 3-in.-square Ducts with Data from 1- and 2-in.-square Ducts

Macromixing Distance/Duct Width								
Duct velocity	Volume flow ratio	Mass velocity ratio	3-in. duct, opposed jets	3-in. duct, single jets	2-in. duct, opposed jets	2-in. duct, single jets	1-in. duct, opposed jets	
50	1:12.5	4.0	2.83	3.13			1.3	
50	1:25	2.0	2.30	6.00		6.20	1.2	
50	1:50	1.0	4.60				3.1	
50	1:50	8.25	2.30	3.41	1.7	3.54		
50	1:50	4.2	2.30	4.00	1.3	5.20		
50	1:25	16.0	1.24	2.00	0.75			
50	1:25	8.2	1.24	2.95	1.20	3.04		
50	1:12.5	16.4	0.31	2.22	0.58			
12.7	1:50	7.75	4.60		2.67			
12.7	1:50	3.9			2.10			
12.7	1:25	7.75	2.30		1.20	3.50		
12.7	1:25	4.0	2.30		2.30	4.1		
12.7	1:12.5	16.0	0.65		0.87			

avoid this, in a small number of tests the sidestream carbon dioxide was introduced through a slit extending over the whole width of the duct.

**PENETRATION DISTANCE.** In general, the  $P/D$  values for the rectangular and square side tubes could be correlated in the same form of equation as for the tube jets, Equation (4a).  $K_p$  values were obtained from the data by the method of least squares and are compared with the result for a cylindrical side tube:

Configuration	$K_p$
Air → 	0.9
→ 	0.9
→ 	1.1
→ 	1.2

The square tube and the rectangular tube placed with the short side perpendicular to the main gas stream produce the smallest penetration distance, followed by the cylindrical tube and the rectangular tube with the long side perpendicular to the main flow. The results agree qualitatively with the conclusions of references 1, 3, and 8.

A simplified, dynamic analysis of the bending of a rectangular jet predicts that the penetration distance, for jets of the same cross-sectional area, should be shorter for the rectangular jet with the short side perpendicular to the main gas flow than for the jet placed transversely. This is supported by the experimental results. The cylindrical- and square-jet penetration distances should lie somewhere between the two extremes if break-up of the jet boundaries by turbulent diffusion were not important. It is clear from these results and the shadowgraph (Figure 1) that the effect of turbulence on the side jet cannot be neglected.

The results of mixing when the side-stream enters from a slit extending over the whole width of the main duct show that, not unexpectedly, a thin sheet of carbon dioxide is easily bent and the penetration distance is very much larger than, for example, for a cylindrical-tube jet.

**BULK MIXING DISTANCE.** For values of  $R_m < 6$ , and for all the  $R_s$  values studied, the cylindrical-tube jet produces about 25% longer bulk mixing distances than the rectangular or square ports. For the higher  $R_m$  values the distances for the cylindrical-tube jet approach closely those for the rectangular and square ports. Just as for the cylindrical side tubes, the data could not be correlated by Equation (6).

**MACROMIXING DISTANCE.** In Figure 11 the macromixing-distance results are presented. The reversal of  $M/D$  variation

with  $R_m$  and  $R_s$ , described previously in connection with the cylindrical-side-tube data, is particularly evident for the rectangular and square side tubes. The reversal appears to occur at smaller  $R_m$  and  $R_s$  values for the rectangular side tubes than for the cylindrical side tubes, especially in the case of the rectangular side tube with its long side perpendicular to the main air stream. The reversal already occurs at an  $R_s$  of 1 : 25 and  $R_m$  of 7.

A qualitative comparison between the different side tubes studied may be made. The cylindrical tube jets consistently produce the shortest macromixing distances, followed by the square tube jets, the rectangular tube with the

short side perpendicular to the main stream, and the rectangular tube with the long side perpendicular to the air stream in increasing order of distance required. A slit extending over the width of the duct requires longer macromixing distances than do the other side tubes used.

**QUALITY OF MICROMIXING.** A comparison between the various kinds of sidestream jets is given in Table 3. The results for the rectangular and square jets indicate that  $R_m$  has a more important influence on micromixing than  $R_s$  does. At lower  $R_s$  ratios of 1 : 50 and 1 : 25 the rectangular-tube transverse to the air stream produces the best micromixing followed closely by the other orientation

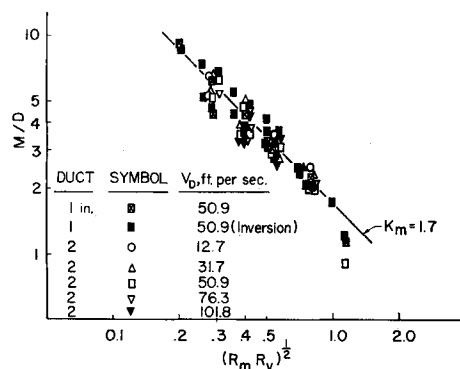


Fig. 9. Correlation of macromixing distance: duct width with mass velocity and volume flow ratios, 1- and 2-in. square ducts, cylindrical side tube.

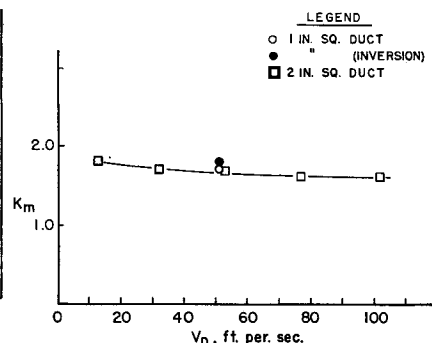


Fig. 9a.  $K_m$  as a function of duct velocity and duct size.

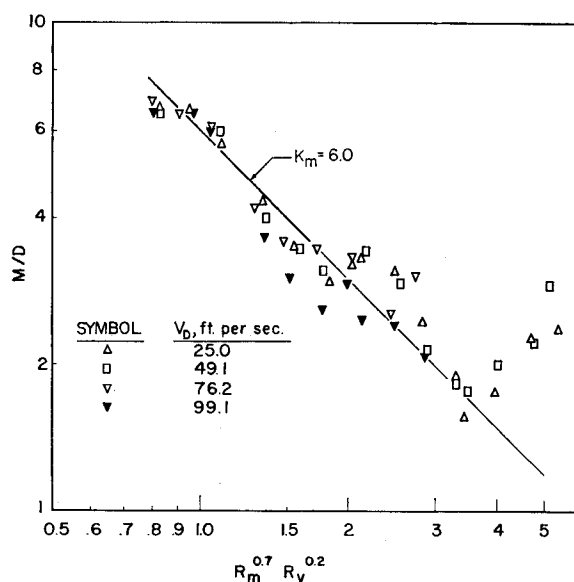


Fig. 10. Correlation of macromixing distance: duct width with mass velocity and volume flow ratios, 3-in. square duct, cylindrical side tube.

and then the square tube in decreasing order of quality. At higher  $R_v$  values,  $\geq 1:12.5$ , the square tube or the rectangular tube with the short side perpendicular to the air stream is best, followed by the rectangular tube with the long side perpendicular to the air stream.

The cylindrical-tube jet mostly produces the poorest micromixing of all the configurations studied, just the opposite of the macromixing situation. The rectangular side tube with the short side perpendicular to the main gas stream consistently gives good mixing; it never is worse than second best of the arrangements studied. If good macromixing is desired, a cylindrical side tube should be used. If good micromixing is required, the rectangular side tube in general is recommended, oriented in a sense dictated by the  $R_m$  and  $R_v$  conditions if possible or with the short side perpendicular to the mainstream.

It was predicted that if the carbon dioxide stream were made to enter from a slit extending from one side wall to the other, the air would have to break through the carbon dioxide barrier in order to proceed. This should be favorable to mixing. Actually, although such a slit produces better micromixing quality than the tube jet, it does not show any advantage over the rectangular or square side tubes.

#### Sampling Studies

In the 3-in.-square duct, at a constant duct velocity of 25 ft./sec. and  $R_v$  of 1:25, sampling traverses were made at  $R_m$  values of 2.2, 9.0, and 17.5.

The duct cross section was divided into nine equal squares and the samples were taken in the center of each:

	Left	Center	Right
Top	1	2	3
Middle	4	5	6
Bottom	7	8	9

Shadowgraphs were taken for comparison in the horizontal and vertical planes at each of the conditions studied by the sampling technique.

The sampling data are presented in Figures 12, 13, and 14 as  $R_s$ , the ratio of the concentration of carbon dioxide in the sample to the total concentration of carbon dioxide flowing in the duct, vs. the distance down the duct. The designations *left side*, *center*, and *right side* and *top*, *middle*, and *bottom* third in the figures refer to the particular portion of the duct involved, as shown above.

In confirmation of the shadow method, there was no carbon dioxide detected by

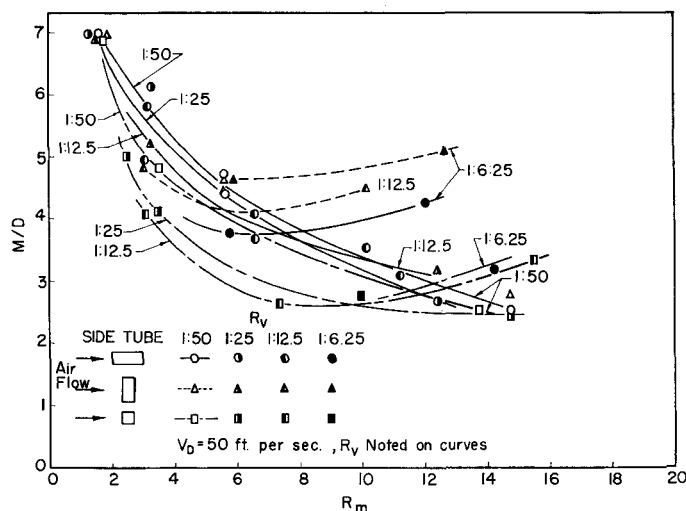


Fig. 11. Macromixing distance: duct width as a function of mass velocity and volume flow ratios, 2-in. square duct, rectangular and square side tubes.

the sampling technique in the vicinity of the entering jet where no schlieren were observed. Also, when the shadowgraph showed an even distribution or disappearance of schlieren, the sampling technique indicated that the carbon dioxide concentration was approximately uniform across the duct.

From Figures 12, 13, and 14, a three-

dimensional picture may be obtained of the mechanism by which the sidestream jet mixes with the main stream. When the high-velocity jet at  $R_m$  of 17.5 strikes the opposite wall, it spreads out across the top, depleting the carbon dioxide concentration in the center of the top section. The gas reaching the side walls

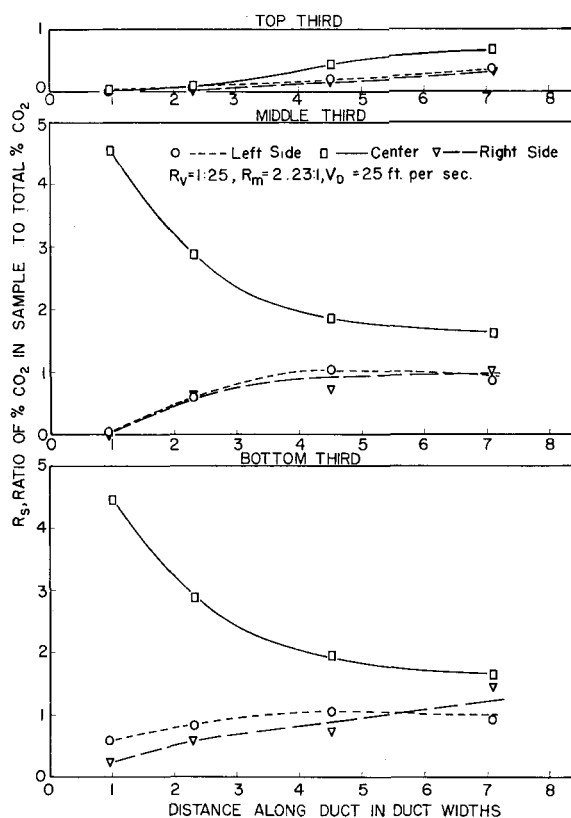


Fig. 12. Ratio of percentage of carbon dioxide in sample to total percentage of carbon dioxide vs. distance along duct, 3-in. square duct, cylindrical side tube.



and then gradually fills the center of the duct. After this occurs, the slower micromixing takes place. At an  $R_m$  of 9.0, the mechanism is much the same except that the distances required to accomplish these phases of mixing are much longer, as is readily seen from Figure 13.

At an  $R_m$  of 2.2, when the sidestream jet is at a low velocity, the situation is different. Here there is a problem of carrying the sidestream gas to the upper portions of the duct. Also, rather than a depletion there is an excess in the center sections of the duct. Mixing takes place by virtue of the turbulence present without any assistance from mechanical distribution.

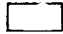



The correlation between the sampling method and the shadowgraphic technique is further illustrated in Table 4. Average  $R_s$  values are given here. *Top* means the average  $R_s$  over left top, center top, right top, etc. It may be seen here that mixing in the horizontal plane is better than mixing in the vertical plane.

#### SUMMARY

By means of shadowgraph and probe sampling techniques, a description has been given of the manner in which a gas flowing in a square duct mixes with a secondary gas introduced sidewise. Mixing is described in terms of the mixing parameters—penetration distance  $P$ , bulk mixing distance  $B$ , macromixing distance  $M$ , and the quality of micromixing. These parameters may be expressed as functions of duct diameter  $D$ , mass velocity ratio  $R_m$ , and volume flow ratio  $R_v$  (sidestream : mainstream) of the two gases.

Experimental penetration-distance data are correlated by  $P/D = K_p/R_m^2 R_v$ , independently of gas density ratio. The constant  $K_p$  increases with duct size for ducts greater than 2-in. square and decreases slightly with increasing duct velocity. A rectangular side tube with the short side perpendicular to the main gas stream or a square side tube gives the shortest penetration distance, followed by the cylindrical side tube, the rectangular side tube with the long side

TABLE 3.  
RECTANGULAR-SLIT MIXING STUDIES,  
QUALITY OF MICROMIXING VS. SLIT CONFIGURATION  
Mixing of Air Flowing in a 2-in. Square Duct with Carbon Dioxide Entering Sidewise from Rectangular Slit; Air Velocity, 50 ft./sec.

$R_v$	$R_m$	Slit configuration			
		→ 	→ 	→ 	→ 
1:50	16	<i>B</i>	<i>B</i>	<i>B</i>	—
	8	—	—	—	<i>C</i>
	6	<i>B</i>	<i>B</i>	—	—
	4	<i>C</i>	<i>B</i>	<i>C</i>	<i>C/D</i>
	2	<i>D</i>	<i>D</i>	<i>D</i>	<i>D</i>
1:25	16	<i>A</i>	—	—	—
	11	—	<i>A/B</i>	—	—
	8	<i>B</i>	—	<i>C</i>	<i>C/D</i>
	4	<i>C/D</i>	<i>C/D</i>	<i>C/D</i>	<i>D</i>
	2	<i>D</i>	<i>D</i>	<i>C/D</i>	<i>D</i>
1:12.5	16	—	—	<i>B</i>	—
	11	<i>B</i>	<i>B</i>	—	—
	8	—	—	<i>C</i>	<i>C/D</i>
	6	<i>C</i>	<i>D</i>	—	—
	4	—	—	—	<i>D</i>
	3	<i>C</i>	<i>C/D</i>	<i>C</i>	—
	2	—	—	—	<i>D</i>
	16	—	—	—	—
1:6.25	12	<i>C</i>	<i>C</i>	<i>B/C</i>	—
	8	—	—	—	<i>D</i>
	6	<i>C/D</i>	<i>D</i>	<i>C/D</i>	—
	4	—	—	—	<i>D</i>
	2	—	—	—	<i>D</i>
	16	—	—	—	—

perpendicular to the main stream, and the slit extending from side wall to side wall of the main duct, in increasing order of penetration distance.

$B/D$  cannot be correlated by any simple mathematical relation, although generally it decreases with an increase in  $R_m$  and  $R_v$  independently of duct size and duct velocity. For  $R_m < 6$ , the cylindrical-tube jet produces longer bulk mixing distances than the rectangular- or square-tube jets. Above an  $R_m$  of 6 the distances required for all jets are about the same.

Experimental macromixing-distance data for the 1- and 2-in. square ducts for  $R_m \leq 8$  over the range of  $R_v$  1:50 to 1:6.25 can be correlated by  $M/D = K_m/(R_m R_v)^{1/2}$  independently of gas-density

ratio. A limitation of  $R_v \leq 1:25$  at  $R_m \leq 8$  must be applied for rectangular or square side tubes.  $K_m$  is independent of duct velocity and size in this range. For the 3-in. square duct the macromixing data for  $R_m \leq 8$  or  $R_v \leq 1:25$  are correlated by  $M/D = K_m/R_m^{0.7} R_v^{0.2}$  where  $K_m$  is independent of duct velocity. The effect of gas-density ratio was not established at this scale.

Above the limiting values of  $R_m$  and  $R_v$  mentioned,  $M/D$  no longer decreases with an increase in  $R_m$  and  $R_v$  and the data cannot be correlated by the given equations. At sufficiently high values of  $R_m$  and  $R_v$ ,  $M/D$  increases with an increase in  $R_m$  and  $R_v$ .

The shortest macromixing distances are obtained with two opposed cylindrical

TABLE 4. SAMPLING STUDY, MIXING OF AIR FLOWING IN 3-INCH SQUARE DUCT WITH CARBON DIOXIDE ENTERING SIDWISE FROM A TUBE

$$R_v = 1:25$$

$$V_D = 25 \text{ ft./sec.}$$

$R_m$	$M/D$	Macromixing							Micromixing						
		Average $R_s$							Average $R_s$						
		Top	Middle	Bottom	Left	Center	Right	Quality	Top	Middle	Bottom	Left	Center	Right	
2.2	6.7	0.45	1.20	1.30	0.80	1.30	0.90	<i>D</i>	0.45	1.20	1.30	0.85	1.30	0.90	
9.0	3.1	0.90	1.15	0.59	1.20	0.40	1.10	<i>C</i>	0.85	1.00	1.05	1.00	1.00	0.95	
17.5	1.8	0.85	0.65	1.05	1.05	0.42	1.10	<i>C</i>	0.95	1.30	1.20	1.00	1.00	1.10	

side tubes, followed in increasing order of required distance by a single cylindrical side tube, the square side tube, the rectangular side tube with the short side perpendicular to the main stream, and the rectangular side tube with the long side perpendicular to the mainstream. Macromixing with a slit extending from side wall to side wall is poorer than with the other side tubes.

The quality of micromixing improves

with an increase in  $R_m$ , duct size, and duct velocity and with a decrease in  $R_s$ . It is observed that velocity ratio rather than mass-flow ratio is the decisive parameter for micromixing. A rectangular side tube with its short side perpendicular to the mainstream consistently gives good mixing. The cylindrical tube produces the worst quality of micromixing. Mixing with a cylindrical tube may be improved by using opposed sidestream

jets. A slit is also superior to a single cylindrical tube.

In general, the sampling studies confirm the picture of mixing obtained with the shadowgraph technique.

#### ACKNOWLEDGMENT

The authors wish to express appreciation to the Pratt and Whitney Aircraft Corporation for providing the funds for this research.

#### NOTATION

$B$  = bulk mixing distance  
 $d$  = diameter of side duct  
 $D$  = diameter of main duct  
 $K_b$  = constant in bulk-mixing-distance correlation  
 $K_m$  = constant in macromixing-distance correlation  
 $K_p$  = constant in penetration-distance correlation  
 $M$  = macromixing distance  
 $P$  = penetration distance  
 $R_m$  = mass velocity ratio, sidestream : main stream  
 $R_s$  = ratio of concentration of  $\text{CO}_2$  in sample to total concentration of  $\text{CO}_2$  flowing in duct  
 $R_v$  = volume flow ratio, sidestream : main stream  
 $S$  = distance downstream of jet entrance  
 $u$  = sidestream-jet-port velocity  
 $V_D$  = average main-duct velocity  
 $\rho$  = density

#### Subscripts

$d$  = sidestream  
 $D$  = main stream

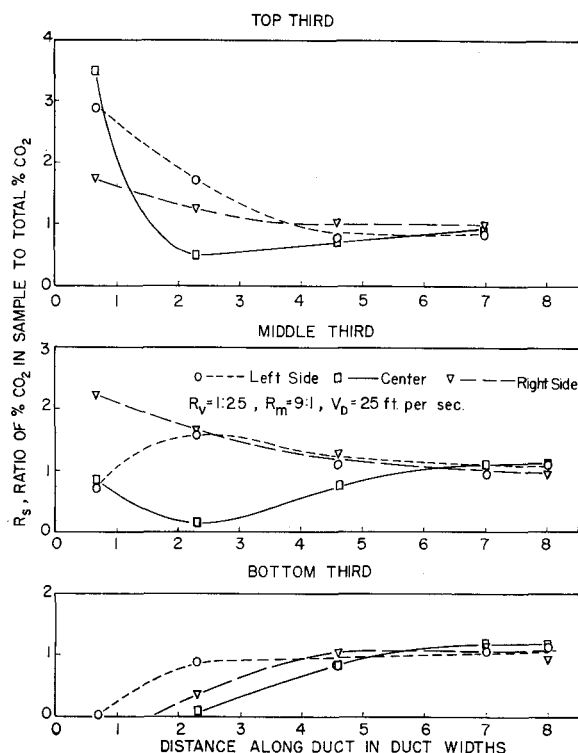


Fig. 13. Ratio of percentage of carbon dioxide in sample to total percentage of carbon dioxide vs. distance along duct, 3-in. square duct, cylindrical side tube.

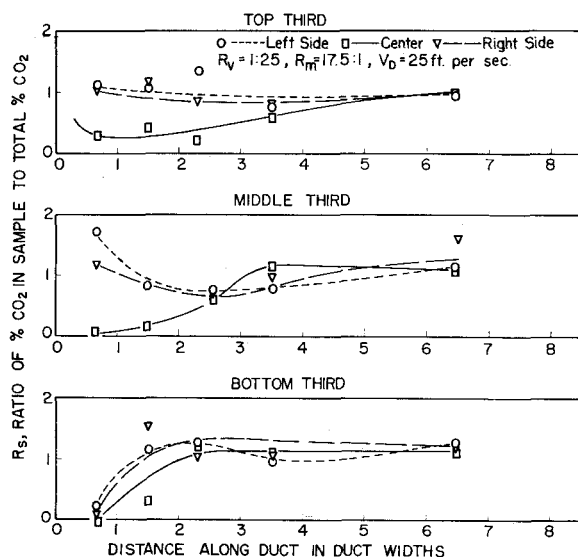


Fig. 14. Ratio of percentage of carbon dioxide in sample to total percentage of carbon dioxide vs. distance along duct, 3-in. square duct; cylindrical side tube.

#### LITERATURE CITED

- Callaghan, E. E., and R. S. Ruggeri, *Natl. Advisory Comm. Aeronaut. Tech. Note* 1615 (June 1948).
- Callaghan, E. E., and D. T. Bowden, *ibid.*, 1947 (Sept. 1949).
- Callaghan, E. E., and R. S. Ruggeri, *ibid.*, 2466 (1951).
- Chilton, T. H., and R. P. Genereaux, *Trans. Am. Inst. Chem. Engrs.*, **25**, 102 (1930).
- Cleaves, V., and L. M. K. Boelter, *Chem. Eng. Progr.*, **43**, 123 (1947).
- Ehrich, F. F., *J. Aeronaut. Sci.*, **20**, 99 (1953).
- Frazer, J. P., *ibid.*, **21**, 59 (1954).
- Hawthorne, W. R., G. F. C. Rogers, and B. Y. Zaczek, *Roy. Aircr. Est. Tech. Note Eng.* 271 (March 1944).
- Kalinske, A. A., and C. L. Pien, *Ind. Eng. Chem.*, **36**, 220 (1944).
- Kuethe, A. M., *J. Applied Mech.*, **2**, A87 (1935).
- Prandtl, L., *Z. angew. Math. Mech.*, **5** (2) 136 (1925).
- Reichardt, H., *ibid.*, **21**, 257 (1941).
- Ruggeri, R. S., E. E. Callaghan, and D. T. Bowden, *Natl. Advisory Comm. Aeronaut. Tech. Note* 2019 (Feb. 1950).
- Ruggeri, R. S., *ibid.*, 2855 (Dec. 1952).